Constraints on the charged Higgs sector from the Fermilab Tevatron collider data

Monoranjan Guchait* and D. P. Roy†
Theoretical Physics Group, Tata Institute of Fundamental Research, Homi Bhabha Road, Mumbai 400 005, India
(Received 30 October 1996)

The top quark data in the lepton plus τ channel offers a viable probe for the charged Higgs boson signal. We analyze the recent Collider Detector at Fermilab data in this channel to obtain a significant limit on the $H^{\pm}$ mass in the large tanβ region. [S0556-2821(97)00211-7]

PACS number(s): 14.80.Cp, 13.35.Dx, 13.85.Ni, 14.65.Ha

The discovery of the top quark signal at the Fermilab Tevatron collider [1,2] has generated a good deal of current interest in the search of new particles in top quark decay. The large mass of the top quark offers the possibility of carrying on this search to a hitherto unexplored mass range for these particles. In particular the top quark decay is known to provide by far the best discovery limit for such a new particle, i.e., the charged Higgs boson [3] of the minimal supersymmetric standard model (MSSM). The signature of the charged Higgs boson in top quark decay is based on its preferential coupling to the τ channel in contrast to the universal W boson coupling. Thus a departure from the universality prediction can be used to separate the charged Higgs boson signal from the W background in

$$t\to bH(bW)\to b\tau\nu. \tag{1}$$

In particular, the top quark decay into the τ lepton channel provides a promising signature for the charged Higgs boson in the region

$$\tan\beta\gtrsim m_t/m_b, \tag{2}$$

where tanβ denotes the ratio of the vacuum expectation values of the two Higgs doublets in MSSM.

In this note we shall analyze the recent Collider Detector at Fermilab (CDF) data on $t\bar{t}$ decay events in the $\ell\tau$ channel, where ℓ denotes e and μ [2,4,5]. This channel has the advantage of a low background. As we shall see below, the number of $t\bar{t}$ events in this dilepton channel relative to the ℓ + multijet channel gives a significant lower bound on the $H^{\pm}$ mass in the large tanβ region (2).

In the diagonal Kobayashi-Maskawa (KM) matrix approximation, the charged Higgs boson couplings to the fermions are given by

$$\mathcal{L}=\frac{g}{\sqrt{2}m_W}H^+\{\cot\beta m_{ui}\bar{u}_i d_{iL}+\tan\beta m_{di}\bar{u}_i d_{iR} + \tan\beta m_{\ell i}\bar{\nu}_i \ell_{iR}\}+\text{H.c.}, \tag{3}$$

where the subscript i denotes quark and lepton generation. The leading log QCD correction is taken into account by substituting the quark mass parameters by their running masses evaluated at the $H^{\pm}$ mass scale [6]. The resulting decay widths are

$$\Gamma_{t\to bW}=\frac{g^2}{64\pi m_W^2 m_t}\lambda^{1/2}\left(1,\frac{m_b^2}{m_t^2},\frac{m_W^2}{m_t^2}\right) \times[m_W^2(m_t^2+m_b^2)+(m_t^2-m_b^2)^2-2m_W^4], \tag{4}$$

$$\Gamma_{t\to bH}=\frac{g^2}{64\pi m_W^2 m_t}\lambda^{1/2}\left(1,\frac{m_b^2}{m_t^2},\frac{m_H^2}{m_t^2}\right)[(m_t^2\cot^2\beta+m_b^2\tan^2\beta) \times(m_t^2+m_b^2-m_H^2)-4m_t^2m_b^2], \tag{5}$$

$$\Gamma_{H\to\tau\nu}=\frac{g^2 m_H}{32\pi m_W^2}m_\tau^2\tan^2\beta, \tag{6}$$

$$\Gamma_{H\to c\bar{s}}=\frac{3g^2 m_H}{32\pi m_W^2}(m_c^2\cot^2\beta+m_s^2\tan^2\beta), \tag{7}$$

where λ denotes the usual Kallen function [3]. They clearly show a large branching fraction for $t\to bH$ decay at tan$\beta\lesssim 1$ and tan$\beta\gtrsim m_t/m_b$, while the branching fraction for $H\to\tau\nu$ decay is $\simeq 1$ at tan$\beta\gg 1$. Thus one expects a large charged Higgs boson signal in top quark decay into the τ channel (1) in the large tanβ region (2).

In the present analysis, we shall concentrate in the tan$\beta\gg 1$ region, for which the charged Higgs boson decays dominantly into $\tau\nu$. The basic process of interest is $t\bar{t}$ production via quark-antiquark (or gluon-gluon) fusion, followed by their decays into charged Higgs or W boson channels: i.e.,

$$q\bar{q}\to t\bar{t}\to b\bar{b}(W^+W^-,W^\pm H^\mp,H^+H^-). \tag{8}$$

The most important $t\bar{t}$ signal is observed in the ℓ + multijet channel [1,2]. It comes from the W^+W^- final state with a branching fraction of 24/81. The corresponding branching fraction from this final state into the $\ell\tau$ channel is only 4/81. However, there would be an additional contribution to the $\ell\tau$ channel from the $W^\pm H^\mp$ final states with a large branching fraction of 4/9, which is to be weighted of course by the ratio $\Gamma_{t\to bH}/\Gamma_{t\to bW}$. Thus a comparison of the number of $t\bar{t}$ events in the two channels leads to an upper limit on this ratio, which can be translated into a lower limit on $H^{\pm}$ mass for a given tanβ.

*Electronic address: guchait@theory.tifr.res.in
†Electronic address: dproy@theory.tifr.res.in

For a quantitative estimate of the above limit, we have to consider the various kinematic cuts and detection efficiencies [2,5]. Our analysis is based on a parton level Monte Carlo simulation of $t\bar{t}$ production using the quark and gluon structure functions of [7]. This is followed by the decays

$$t \to b \not{\ell} \nu, \quad \bar{t} \to \bar{b} q \bar{q}' \tag{9}$$

and vice versa for the $\not{\ell}$ + multijet channel. The quark jets are merged according to the CDF jet cone algorithm of $\Delta R = (|\Delta\eta|^2 + |\Delta\phi|^2)^{1/2} = 0.7$. The resulting final state is required to satisfy the CDF cuts [2]:

$$p_T^{\not{\ell}} > 20 \text{ GeV}, \quad |\eta_{\not{\ell}}| < 1, \quad \not{E}_T > 20 \text{ GeV}, \quad \text{and } n_{\text{jet}} \geq 3$$
$$(\text{with } E_T^j > 15 \text{ GeV}, \ |\eta_j| < 2). \tag{10}$$

We estimate the efficiency factor for these kinematic and topological cuts to be 52% for $m_t = 175$ GeV. This has to be supplemented by the following CDF efficiency factors [2,5,8]:

$$\epsilon_{\text{tr}}^{\not{\ell}} = 0.93, \quad \epsilon_{\text{id}}^{\not{\ell}} = 0.87, \epsilon_{\text{iso}}^{\not{\ell}} = 0.9, \quad \epsilon_b = 0.4, \quad \epsilon_{\text{az}} = 0.85, \tag{11}$$

corresponding to lepton triggering, identification, and isolation cut along with those due to SVX b tagging and azimuthal gaps in the detector. The combined efficiency factor is 12.8%, in reasonable agreement with the CDF estimate of 11.8% [2] including hadronization and a more exact detector simulation.

The measured $t\bar{t}$ cross section from this channel, including SLT b tagging, is [2]

$$\sigma_t = 7.5 \pm 1.5 \text{ pb}. \tag{12}$$

This is 40–50 % higher than the next to leading order QCD prediction for $m_t = 175$ GeV [9]. We shall use this cross section for normalization. Thus our results will be independent of any theoretical model for the $t\bar{t}$ cross section. It will only depend on the preferential $H^{\pm}$ coupling to the τ channel vis-a-vis the universal $W^{\pm}$ boson coupling. It should be noted here that the above cross section corresponds to the WW contribution to the $t\bar{t}$ cross section, represented by the first term of Eq. (8), since any contribution from the other terms would have very small detection efficiency for this channel. These contributions should be included, of course, in a more exact analysis along with the experimental uncertainity in σ_t, which can be best done by the CDF Collaboration.

An alternative normalization prescription is based on using the QCD prediction for the $t\bar{t}$ cross section. In this case one has to consider an additional constraint from the fact that the predicted WW branching fraction of $t\bar{t}$ and hence the $t\bar{t}$ cross section in the hard l + multijet channel goes down rapidly at large $\tan\beta$ in conflict with the experimental value (12). On the other hand, there can be an enhancement of the $t\bar{t}$ cross section by mechanisms beyond the standard model (SM), which should not be ignored while probing beyond SM physics. Our normalization prescription has the advantage of incorporating the former automatically and making allowance for the latter.

TABLE I. The efficiency factors for the $\not{\ell}\tau$ channel corresponding to the indicated kinematical and topological cuts. For the WW process, the corresponding efficiencies from the CDF simulation are shown in parenthesis. The middle column shows the triggering, isolation, and identification efficiencies from the CDF simulation.

Eff. / Process	$p_T^{\not{\ell},\tau}$ and geom.	$\epsilon_{\text{tr}}^{\not{\ell}}, \epsilon_{\text{iso}}^{\not{\ell}}, \epsilon_{\text{id}}^{\not{\ell}}, \epsilon_{\text{id}}^{\tau}$	Jets, H_T and $\not{E}_T$
WW	0.16 (0.13)	0.93×0.9	0.64 (0.54)
$WH(80)$	0.19	$\times\ 0.87 \times 0.5$	0.61
$WH(100)$	0.21	$= 0.36$	0.62
$WH(120)$	0.22		0.64
$WH(140)$	0.22		0.65

The $\not{\ell}\tau$ channel of our interest corresponds to the decays

$$t \to b \not{\ell} \nu, \ \bar{t} \to \bar{b} \tau \nu \tag{13}$$

and vice versa, where the τ lepton coming from $W(H)$ decay has a definite polarization $P_\tau = -1(+1)$. It is identified in its hadronic decay mode as a thin jet containing one or three charged prongs [4,5]. This accounts for a τ branching fraction of about 64% [10]. The dominant contributions come from

$$\tau \to \pi\nu(12\%), \ \rho\nu(25\%), \ a_1\nu(15\%), \tag{14}$$

adding up to a little over 80% of the hadronic τ decay. We shall combine these three decay modes and scale up their sum by 20% to simulate hadronic τ decay. The decay distributions are simply given by [11]

$$\frac{d\Gamma_\pi}{\Gamma_\pi d\cos\theta} = \frac{1}{2}(1 + P_\tau \cos\theta), \tag{15}$$

$$\frac{d\Gamma_v}{\Gamma_v d\cos\theta} = \frac{1}{2}\left(1 + \frac{m_\tau^2 - 2m_v^2}{m_\tau^2 + 2m_v^2} P_\tau \cos\theta\right), \ v = \rho, a_1, \tag{16}$$

where θ is the direction of the decay hadron in τ rest frame relative to the τ line of flight. It is related to the fraction x of τ momentum carried by the hadron:

$$\cos\theta = \frac{2x - 1 - m_{\pi,v}^2/m_\tau^2}{1 - m_{\pi,v}^2/m_\tau^2}. \tag{17}$$

This decay hadron momentum is refered to below as p^τ.

The resulting final state is required to satisfy the CDF kinematic cuts [4,5],

$$p_T^{\not{\ell}} > 20 \text{ GeV}, \ |\eta_{\not{\ell}}| < 1, \ p_T^\tau > 15 \text{ GeV}, \ |\eta_\tau| < 1.2. \tag{18}$$

The corresponding efficiency factors are shown in the first column of Table I for the WW and WH contributions with different charged Higgs boson masses. It includes the hadronic branching fraction of τ along with a factor of 0.8 due to azimuthal gaps in the detector, resulting in 15%(5%) loss to $\not{\ell}(\tau)$ detection efficiency [8]. The opposite polarizations of τ coming from W and H decays results in a somewhat larger efficiency factor for the latter, which increases further with increasing H mass. The second column shows the CDF efficiency factors for the lepton trigger, isolation, and identifi-

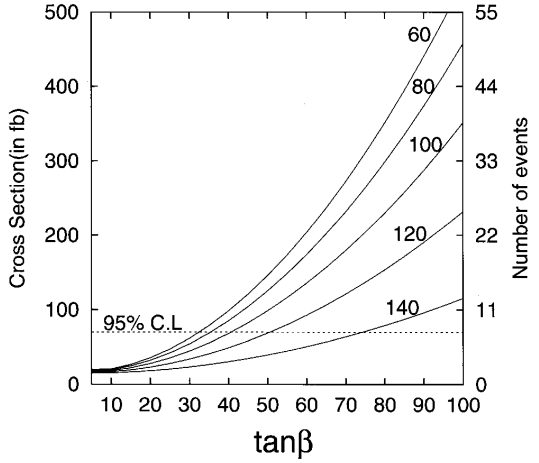

FIG. 1. The predicted cross section (No. of events for 110 pb^{-1} luminosity) shown against tanβ for different $H^{\pm}$ masses. The 95% C.L. limit corresponding to 7.7 events is shown as a dashed line.

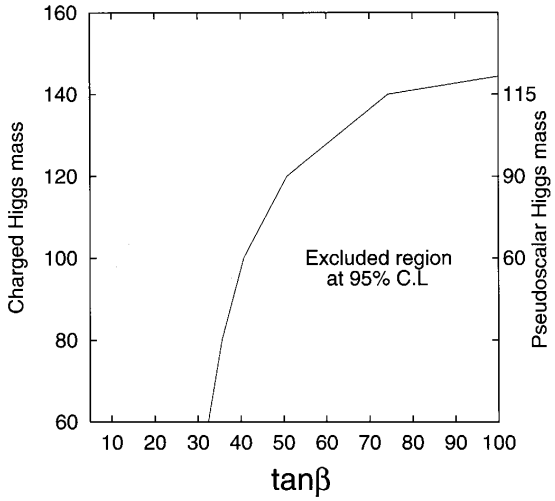

FIG. 2. The 95% C.L. exclusion contour in the $H^{\pm}$ mass and tanβ plane. The corresponding pseudoscalar mass m_A is indicated on the right.

cation as well as the τ identification. These are expected to be essentially process independent. The last column shows the efficiency factors for the topological and missing-E_T cuts [4,5]:

$$n_{\mathrm{jet}} \geq 2 \quad (\text{with } E_T^j > 10 \text{ GeV}, \ |\eta_j| < 2), \tag{19}$$

$$H = p_T^{\not\ell} + p_T^{\tau} + \not{E}_T + \sum_j E_T^j > 180 \text{ GeV}, \tag{20}$$

$$\sigma_{\not{E}_T} = \not{E}_T / \sqrt{p_T^{\not\ell} + p_T^{\tau} + \sum_j E_T^j} > 3 \ \mathrm{GeV}^{1/2}. \tag{21}$$

For the WW contribution, the efficiency factors for the kinematic and topological cuts from the CDF simulation [5] are shown in parentheses for comparison. For both cases they are 15–20% below our Monte Carlo (MC) estimates, which indicate an overall error of $\sim$30% in our MC result.

The product of the efficiency factors in the three columns of Table I gives the overall acceptance factor for the $\not\ell\tau$ channel. This is to be multiplied by the branching fraction of 4/81 for the WW contribution and 4/9 times $\Gamma_{t\to bH}/\Gamma_{t\to bW}$ for the WH. The resulting factor gives the corresponding $\not\ell\tau$ cross section as a fraction of the σ_t of Eq. (12).

Figure 1 shows the predicted cross section in the $\not\ell\tau$ channel against tanβ for several charged Higgs boson masses. The scale on the right shows the corresponding number of events for the accumulated CDF luminosity of 110 pb^{-1}. The prediction includes the WW contribution of 14 fb, i.e., 1.5 events. The corresponding number from the CDF simulation is 1.2 events [5,8]. It may be noted that the dominant contribution comes from WW for tan$\beta = 5-10$, where the $t\to bH$ width has a pronounced dip. However, the WW is overwhelmed by the WH contribution, when kinematically allowed, for tan$\beta \gtrsim m_t/m_b$. The preliminary CDF data shows four events in this channel against a background of 2 ± 0.4 [2,4,5]. The corresponding 95% C.L. limit of 7.7 events [10,12] is indicated in the figure. This implies a $H^{\pm}$ mass limit of 100 GeV for tan$\beta \geq 40$, going up to 120 GeV for tan$\beta \geq 50$. One may scale down the predicted cross section by 30% to account for the difference between the acceptance factors of the CDF simulation and ours. This would correspond to an upward shift of the above tanβ limit by about 10 units for a given $H^{\pm}$ mass. Nonetheless it would still represent a very significant constraint on the charged Higgs boson mass in the large tanβ region.

The mass limits of Fig. 1 for different values of tanβ are converted into a 95% exclusion contour in the $m_H - \tan\beta$ plane in Fig. 2. As mentioned above, a 30% reduction in the signal cross section would correspond to a rightward shift of this contour by roughly 10 units in tanβ. The scale on the right shows the corresponding Higgs pseudoscalar mass m_A from the MSSM mass relation $m_{H^{\pm}}^2 - m_A^2 = m_W^2$ at the tree level [13]. The radiative correction to this mass relation is known to be no more than a few GeV. One sees from this figure that a relatively light pseudoscalar mass ($m_A \leq 60$ GeV) is disallowed for tan$\beta \geq 40$. It is precisely in this region of m_A and tanβ that one expects to get a significant radiative correction to R_b ($\Gamma_z^b/\Gamma_z^{\mathrm{had}}$) from the Higgs sector of MSSM [14]. Thus the so-called large tanβ solution to the (so-called) R_b anomaly seems to be strongly disfavored by the above CDF data.

Recently the CDF collaboration has obtained a limit on the charged Higgs mass in the large tanβ region [15] on the basis of their analogous data in the inclusive τ channel. Thus it is instructive to compare the relative merits of the two channels for probing the charged Higgs signal. The inclusive τ channel corresponds to a larger branching fraction than the $\not\ell\tau$ channel analyzed here. However, it is compensated by much stronger experimental cuts, required to control the background. Consequently, the final signal cross section in the inclusive τ channel is similar to that in the $\not\ell\tau$ channel. This can be seen by comparing the predicted cross sections in the two channels in the region of tan$\beta = 5-10$. The reason we get a much larger signal cross section in the large tanβ region compared to [15] and hence a stronger mass limit is due to the different normalization procedure followed in the two cases. We use the $t\bar{t}$ cross section in the WW

decay mode as measured via the lepton plus $\geqslant 3$ jets channel for our normalization, while the QCD prediction for the inclusive $t\bar{t}$ cross section is used for normalization in [15]. The former method is evidently more powerful in the large $\tan\beta$ region as discussed earlier.

It should be noted here that even with stronger cuts the number of estimated background events in the inclusive τ channel are five times larger than in the $\ell\tau$ channel, for equal luminosity [5,15]. Thus the $\ell\tau$ channel will be clearly more advantageous at the Tevatron upgrade, which promises a 20 times higher luminosity along with a $\sim 40\%$ larger $t\bar{t}$ cross section [9]. In particular the $\ell\tau$ channel with b tagging seems to be practically free from nontop quark background [4,5]. The main background in this case is from the $t\bar{t}$ decay via the WW mode. This can be suppressed relative to the $H^{\pm}$ signal by exploiting the opposite polarizations of τ lepton in the two cases [16]. Thus the $\ell\tau$ channel with b tagging is best suited for the charged Higgs boson search at the Tevatron upgrade as well as the CERN Large Hadron Collider (LHC).

In summary, the $t\bar{t}$ data in the $\ell\tau$ channel is well suited to probe for a charged Higgs boson signal because of the small background. On the basis of the recent CDF data in this channel we can already get a significant limit on the $H^{\pm}$ mass in the large $\tan\beta$ region. With a much higher luminosity expected at the Tevatron upgrade the probe can be extended over a significantly wider range of $H^{\pm}$ mass and $\tan\beta$.

It is a pleasure to thank Professor M. Hohlmann of the CDF Collaboration and Professor N.K. Mondal of D0 for many helpful discussions.

[1] CDF Collaboration, F. Abe *et al.*, Phys. Rev. Lett. **74**, 2626 (1995); D0 Collaboration, S. Abachi *et al.*, *ibid.* **74**, 2632 (1995).

[2] P. Tipton, in *Proceedings of the 28th International Conference on High Energy Physics*, Warsaw, 1996 (in press).

[3] V. Barger and R.J.N. Phillips, Phys. Rev. D **41**, 884 (1990); A.C. Bawa, C.S. Kim, and A.D. Martin, Z. Phys. C **47**, 75 (1990); R.M. Godbole and D.P. Roy, Phys. Rev. D **43**, 3640 (1991); R.M. Barnett, R. Cruz, J.F. Gunion, and B. Hubbard, *ibid.* **47**, 1048 (1993).

[4] CDF Collaboration, S. Leone *et al.*, in XI Topical Workshop on $\bar{p}p$ Collider Physics, Padova, 1996 (unpublished).

[5] CDF Collaboration, M. Hohlmann *et al.*, in *Topics in Electroweak Physics*, Proceedings of the Lake Louise Winter Institute, Lake Louise, Canada, 1996, edited by A. Astbury *et al.* (World Scientific, Singapore, 1997).

[6] M. Drees and D.P. Roy, Phys. Lett. B **269**, 155 (1991); D.P. Roy, *ibid.* **283**, 403 (1992).

[7] A.D. Martin, R.G. Roberts, and W.J. Stirling, Phys. Lett. B **306**, 145 (1993); **309**, 492 (1993).

[8] M. Hohlmann (private communication).

[9] E. Berger and H. Contoparagos, Phys. Lett. B **361**, 115 (1995); S. Catani *et al.*, *ibid.* **378**, 329 (1996).

[10] Particle Data Group, R. M. Barnett *et al.*, Phys. Rev. D **54**, 1 (1996).

[11] B.K. Bullock, K. Hagiwara, and A.D. Martin, Phys. Rev. Lett. **67**, 3055 (1991); D.P. Roy, Phys. Lett. B **277**, 183 (1992).

[12] O. Helene, Nucl. Instrum. Methods Phys. Res. **212**, 319 (1983).

[13] J.F. Gunion, H.E. Haber, G. Kane, and S. Dawson, *The Higgs Hunters' Guide* (Addison-Wesley, Reading, MA, 1990).

[14] D. Garcia, R. Jimenez, and J. Sola, Phys. Lett. B **347**, 321 (1995); P.H. Chankowski and S. Pokorski, Nucl. Phys. **B475,** 3 (1996).

[15] CDF Collaboration, C. Loomis *et al.*, presented at the DPF Meeting, Minneapolis, 1996 (unpublished).

[16] S. Raychaudhuri and D.P. Roy, Phys. Rev. D **52**, 1556 (1995); **53**, 4902 (1996).